

Simulation Work and Analysis for Proposed Low Energy Neutrino Detector at Oak Ridge National Laboratory

Noah Grethen, University of Chicago

University of Tokyo Research Internship Program, Yokoyama-Nakajima Research Group, Summer 2023

Abstract

In order to measure the charged current $\nu_e-^{16}\text{O}$ and neutral current cross sections, an experiment using a water Cherenkov detector for low energy neutrinos at Oak Ridge National Laboratory is being proposed. To provide insight for this experiment, simulation work was done here. Relevant simulation data and results were obtained regarding the effect of Gd addition, average photomultiplier tube hits and trigger efficiency for gammas, neutrons and electrons generated inside the detector and also the performance of some algorithms for particle discrimination between these three particles. Overall, reasonable detection capability and trigger efficiency could be achieved and using 0.1% by weight Gd in the detector, neutrons could be identified between gammas and electrons using a Cherenkov angle reconstruction/photomultiplier tube hit isotropy algorithm, but a scattering goodness algorithm could not effectively discriminate between gammas and electrons.

1 Motivation and Physics Background 1.2 Neutrino Interactions

First some motivation for measuring low energy neutrino is given along with some of the dominant particle interactions that occur for the energies and detector of interest.

1.1 Supernova Neutrinos

Recently more attention has been given to supernova neutrinos with effective, efficient measurement of them being one focus. Detection and evaluation of supernova relic neutrinos and specific star core-collapse events could help give a better understanding of certain physics such as the mechanism of a supernova. Several different theoretical models exist for supernovas that still ought to be further tested experimentally. Notably SN1987A^[1] has been the only observed supernova event so far but with modern detectors capable of detecting supernova neutrinos like Super-Kamiokande and the future Hyper-Kamiokande, the hope is to record any new nearby supernovae that could provide orders of magnitude more resulting detected neutrinos. In contrast to other neutrino sources, supernova neutrinos are relatively lower energy, in the range of MeV. Considering mainly electron flavor neutrinos in this energy range, inverse beta decay is one of the main modes of interaction. However, other types of interactions still can be seen and ideally they should fully accounted for in neutrino detectors that are in or planned to be in operation. This is where the proposed Oak Ridge experiment mentioned in this report hopes to provide useful additional cross section and other data for these low energy neutrinos and which this report gives background simulation work for. In particular, the planned design of a water Cherenkov detector for Oak Ridge allows for the same detection techniques as Super-K and Hyper-K so the resulting Oak Ridge data hopefully can be fully utilized for these detectors in preparation for a future supernova.

To lay down some insight on the relevant neutrino interactions, it's noted that there are many different types of interactions which depend on the neutrino flavor and detector used but considering a water Cherenkov detector and the Oak Ridge source described later, we primarily will look at the electron neutrino interactions. Particularly of interest is the charged current electron neutrino and oxygen-16 interaction, $\nu_e + ^{16}\text{O} \rightarrow e^- + ^{16}\text{F}^*$, and the neutral current interaction which is similar without the electron neutrino converting into an electron. These are the two main interactions which the Oak Ridge experiment group wishes to measure and analyze. Here, the resulting fluorine (or oxygen) nuclei is recoiled and thus excited, prompting the emission of a gamma or a nucleon. Using a water Cherenkov detector, the CC interaction is therefore expected to be observable via Cherenkov radiation from the resulting electron and gamma (which would need to undergo Compton scattering) while the NC interaction could be detectable with slightly more difficulty given that the additional electron isn't produced. Along with these two interactions, other common reactions in a water Cherenkov detector include inverse beta decay ($\bar{\nu}_e + p \rightarrow e^+ + n$) and neutrino-electron scattering which we would like to separate from the CC and NC above in the experiment at hand.

2 Detector Setup

With some motivation and physics background provided, basic information on the Oak Ridge neutrino source along with the detector configurations for the experiment are now given.

2.1 Neutrino Source

At the SNS (Spallation Neutron Source) in Oak Ridge National Laboratory where the proposed experiment is planned to be, neutrinos are produced alongside neutrons via a pulsed timing

proton beam on a Hg target. Energetic protons incident on the Hg can cause the creation of charged pions. The negative pions often capture on the mercury while positive pions promptly decay, giving electron and muon flavor neutrinos. A benefit of using Hg as the proton beam target is that the positively charged pions/muons usually decay nearly from rest due to the density of the mercury, giving a more coherent energy spectrum. Fig. 1 below gives an expected energy spectra for the resulting neutrinos. Meanwhile, as the proton beam is pulsed, there is good control over the timing.

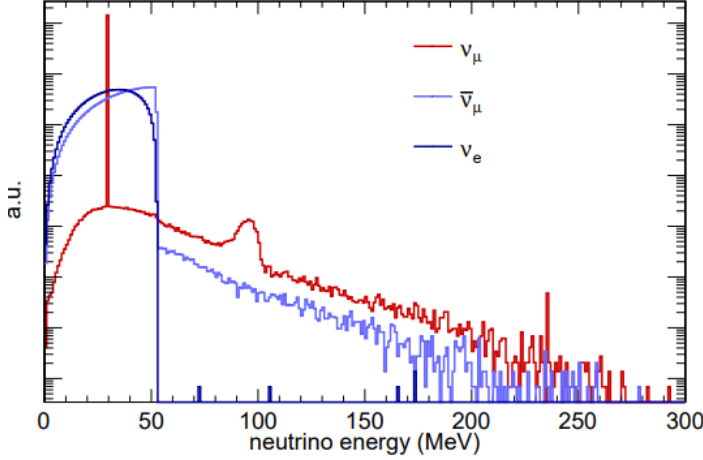


Fig. 1: Simulated neutrino energy of Oak Ridge source.
Figure taken from Ref. [2]

For reference, the positive pion and muon decays considered are,

$$\pi^+ \rightarrow \mu^+ + \nu_\mu$$

$$\mu^+ \rightarrow e^+ + \nu_e + \bar{\nu}_\mu$$

which is the highest branching ratio decay mode for π^+ at BR=0.99998 and likewise the dominant decay mode for μ^+ . Muon flavor neutrinos are produced in addition to electron flavor, but we don't need to care too much about them given that muons are too heavy to significantly interact via CC.

2.2 Software Used and Detector Configurations

Now a quick note on the software is that the Geant4^[3] based WCSim^[4] was used for simulating physics and detector processes while ROOT from CERN was used for data analysis and the graphs shown. For the detector, the geometry and specifications that are considered in the simulations include:

- Cylindrical water Cherenkov detector tank of 3 m in diameter and 2 m in height, filled with pure water
- 3 inch PMTs lining the inside walls of the detector tank, with quantum efficiency the same as the Super-K 20 inch PMTs
- With and without the addition of 0.1% wt Gd in the detector water
- Only 1 inner detector wall, but an outer wall is also being considered outside of this report (to catch escaping gammas)
- With and without PMT dark noise of 300 Hz

- A trigger system (15 ns trigger window, 5 ns pre-trigger window, 50 ns post-trigger window, differing PMT hit thresholds, only first PMT hit taken per PMT per trigger window, no dark noise PMT hit threshold adjustment)

**Note that the detector is relatively quite small and this (as well as the lower energies being looked at) will affect the performance*

With that, from above the number of total PMTs and average dark noise PMT hits for 0.3 kHz dark noise corresponding to a given PC ("PC" meaning photo-coverage which is effectively the percent of inner detector wall surface area covered by photomultiplier tubes) is:

- 8% PC → 7.57% effective PC, 536 total PMTs, avg. dark noise PMT hits = 0.002412
- 15% PC → 14.06% effective PC, 999 total PMTs, avg. dark noise PMT hits = 0.0044955
- 30% PC → 26.5% effective PC, 1984 total PMTs, avg. dark noise PMT hits = 0.008928
- 60% PC → 54.9% effective PC, 3956 total PMTs, avg. dark noise PMT hits = 0.017802
- 78% PC → 69.5% effective PC, 5056 total PMTs, avg. dark noise PMT hits = 0.022752

For clarification, avg. dark noise PMT hits means the average number of PMTs in the detector active in a 15 ns window with a dark noise rate of 0.3 kHz. Effective PC is the actual PC due to the limiting geometry of PMT layout in which the initial exact photo-coverage percent can't be obtained. From now on though, the effective PC won't be used and instead just the initial PC that the program tries to get as close as possible to will be stated.

3 Preliminary Work

Now the effect of the addition of Gd, average PMT hits for an event, and trigger efficiencies are presented. A question to hopefully answer is *What PC and trigger hit thresholds are needed to detect a reasonable number of events and obtain a desired trigger efficiency?*

3.1 Gd

With the initial simulation specifications laid out, the first matter looked into was correctly implementing in simulation the addition of Gadolinium in the detector and investigating whether the expected differences can be seen. Without Gd, a neutron produced inside the detector would most likely capture on a proton from the water via $n + p \rightarrow d + \gamma$ (2.2 MeV) with a mean capture time of around 200 microseconds, given the neutron doesn't escape the detector. Observation of the capture is then possible from the 2.2 MeV gamma undergoing Compton scattering to produce a charged particle which would further produce Cherenkov radiation. However, given that the energy of the gamma is quite low, the event is difficult to detect. That is where Gadolinium can help, making the neutron

more visible as neutron capture on Gd produces multiple gammas (around 2 to 3) with a higher total energy of 8 MeV via $n + {}^N\text{Gd} \rightarrow {}^{N+1}\text{Gd} + \gamma's$ (total 8 MeV). The introduction of Gd can be achieved through Gd salts (such as gadolinium sulfate which is used in the Super-K detector) with appropriate filtration systems. Different percentages of Gd by weight in the water will give differing mean capture times. From here on out, 0.1% wt Gd will be used which gives a mean capture time of around 20 microseconds, with the capture occurring at 90% probability (while the other 10% is mainly proton capture). A note on the Gd mean capture time is that it is still relatively long and can give a timing difference between say a gamma and a neutron produced at the same time.

Below in Fig. 2 are two detector PMT hit plots with and without 0.1% wt Gd using a high 90% PC, “NoTrigger” mode (which captures everything over a long period of time), isotropic and uniform generation in the detector, and no dark noise. The effect of Gd can clearly be noticed.

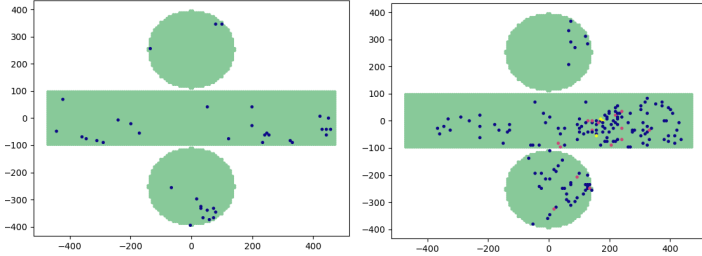


Fig. 2: Neutron event without Gd on the left and with 0.1% wt Gd on the right

Following this in Fig. 3 and Fig. 4 are histograms of the two different capture processes from simulation to ensure they are implemented correctly and to further illustrate the difference, using the same detector settings as above and generating 100,000 neutrons each for both. By just plotting the PMT hit times, one can see the difference in total PMT hits as well as mean capture times which are close to the expected values of 200 and 20 microseconds.

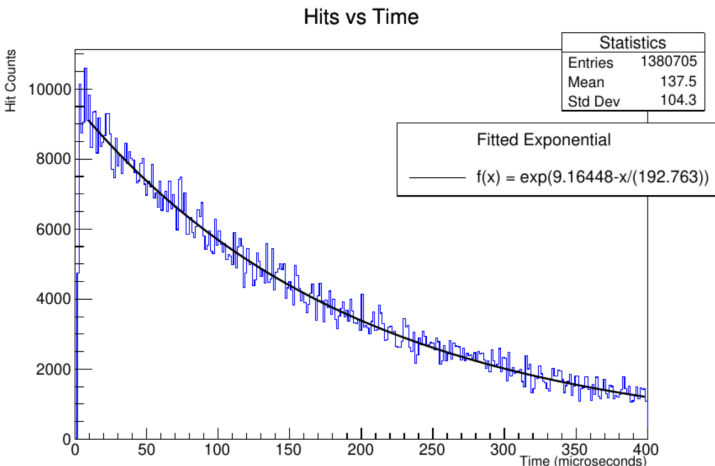


Fig. 3: Neutron capture timing without Gd

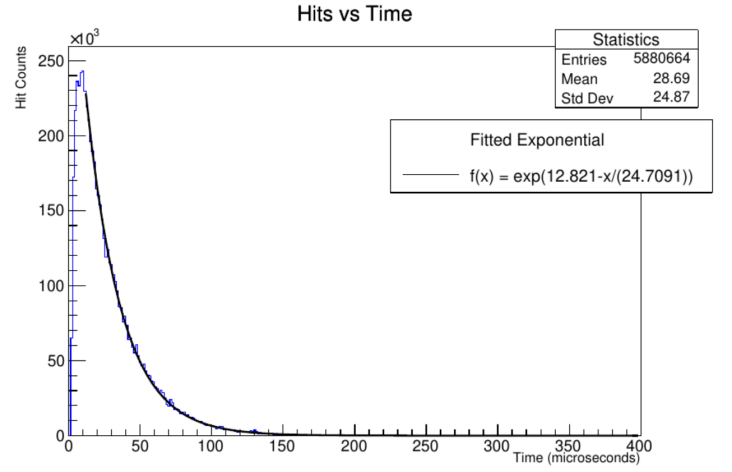


Fig. 4: Neutron capture timing with 0.1% wt Gd

3.2 Average PMT hits

One might now want to know the average number of PMT hits of standard particles we would be seeing in the detector for a given energy and PC. This would help give an idea of what would be possible to work with for analysis later. Thus follows in Figs. 5,6,7 simulation data for neutrons without Gd, neutrons with 0.1% wt Gd, gammas, and electrons. 1,000 events for each PC and energy along with no dark noise, uniform generation in detector were used. Events with no hits were not included in the average PMT hit calculation.

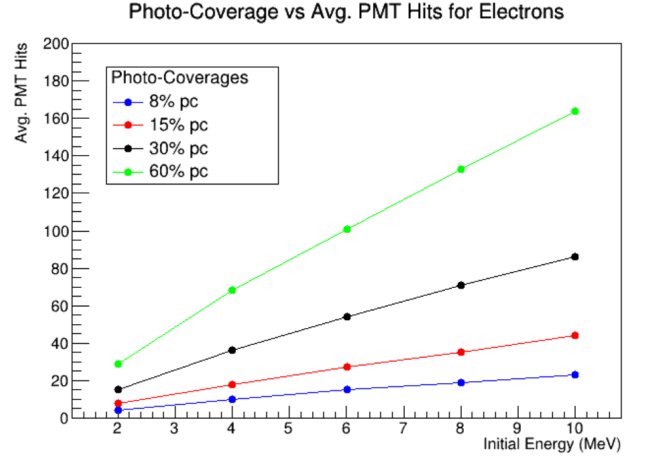


Fig. 5: Electron events

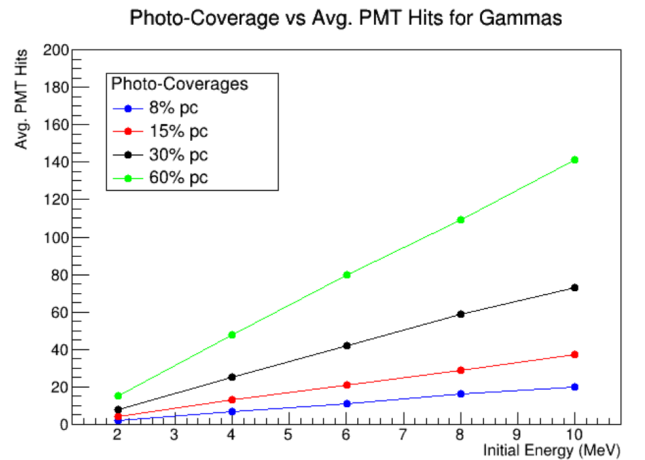


Fig. 6: Gamma events

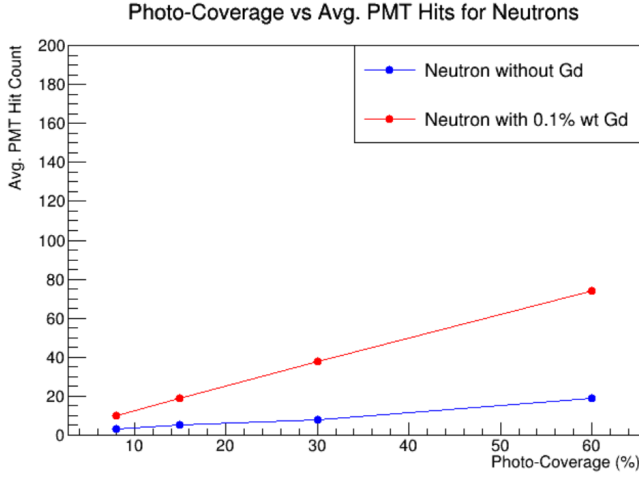


Fig. 7: Neutron events. Different energies for neutrons should give the same values of average hits given that neutrons simply need to thermalize to sub-MeV energies for capture. Therefore energies are not plotted

3.3 Trigger Efficiency

Closely related to the average number of PMT hits per event is a quantity known as the trigger efficiency which is defined here as the number of triggers over the number of generated particles for a set of generated particles. Overall trigger efficiency as the name suggests is as measure of how well we can trigger on events and is dependent on the trigger PMT hit threshold and PC. Figures 8 through 11 give trigger efficiencies for gammas and electrons where in total energies of 2, 4, 6, and 10 MeV along with PC of 8%, 15%, 30%, 60%, and 78% were examined but here in the report, only the 8% and 30% PC plots are shown given the conclusion provided in the next subsection.

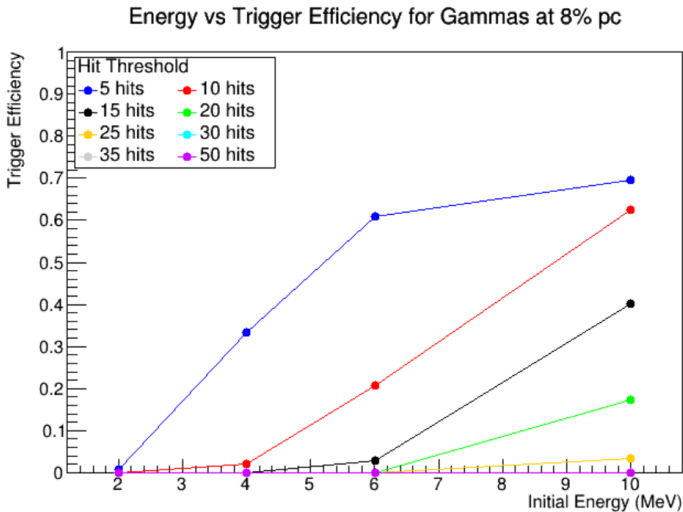


Fig. 8: Gamma events using 8% PC

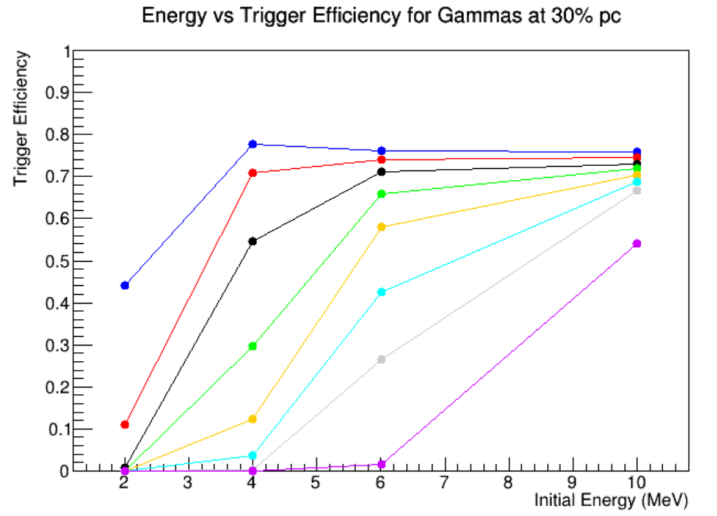


Fig. 9: Gamma events using 30% PC

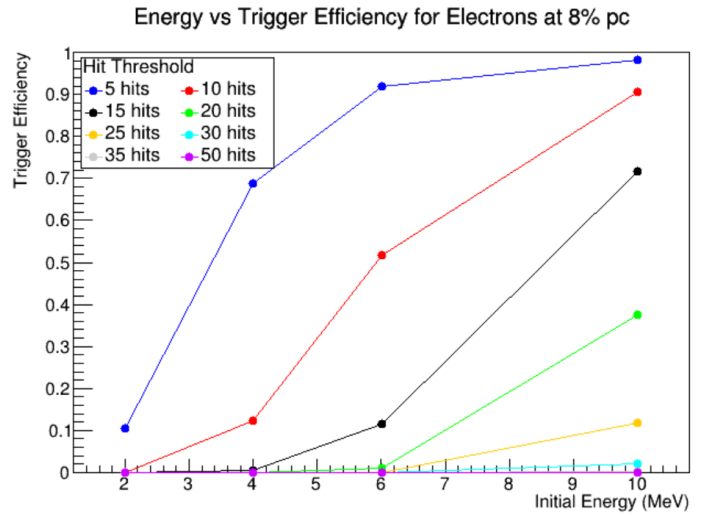


Fig. 10: Electron events using 8% PC

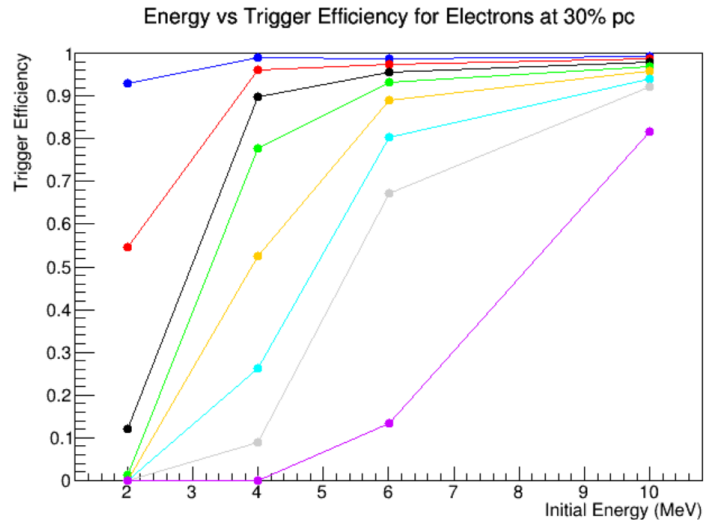


Fig. 11: Electron events using 30% PC

From the above figures, there seems to be a saturation for gammas at around 0.8 on the trigger efficiency you can obtain for the energies and PC considered which carries even into all energies and PMT hit thresholds when using 78% PC. Meanwhile for electrons, there isn't such a saturation as might be expected given electrons in theory ought to be easier to detect than gam-

mas.

Finally below as fig. 12 and 13 are trigger efficiency plots for neutrons without and with Gd. Since only a single energy needed to be considered for neutrons, the plot format for neutrons differs slightly.

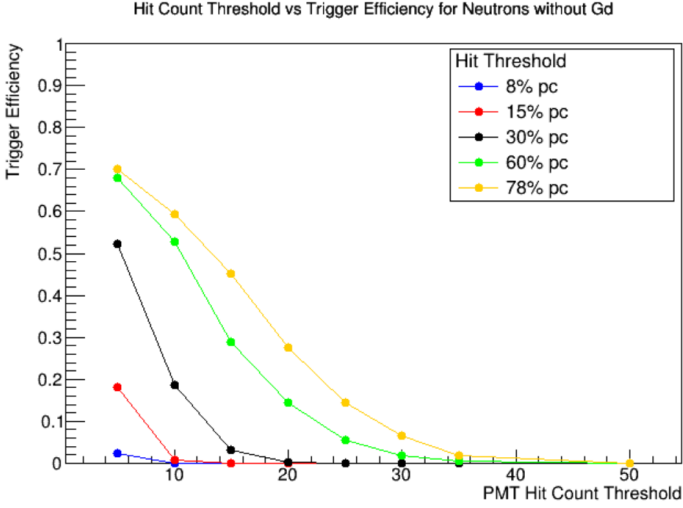


Fig. 12: Neutron events without Gd

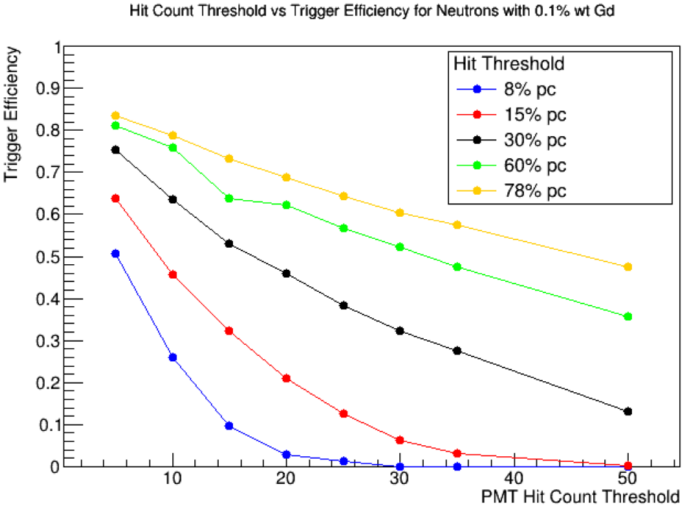


Fig. 13: Neutron events with 0.1% wt Gd

3.4 Section Conclusion

Answering that question from earlier in the section 3 heading of “What PC and trigger thresholds are needed to detect a reasonable number of events and obtain a desired trigger efficiency?”, all together based on the plots above and other PC plots not shown, a 30% PC with 15 hit threshold looked to a suggested set up (assuming unexpected higher dark noise/anything else does not become an issue at the 15 hit threshold mark). This allows for the lowest PC with a desirable 80 to 90 percent trigger efficiency for gammas and electron and reasonable number of PMT hits per event. In particular,

1. **For Electrons:** 90% trigger efficiency in the > 4 MeV range with a possibility of still measuring 2 to 4 MeV at a decreased efficiency.

2. **For Gammas:** Roughly 80% trigger efficiency for energies > 6 MeV with also the possibility of still triggering on 2 to 6 MeV.

3. **For Neutrons with 0.1 Gd added:** A 75% trigger efficiency while for comparison a lower 50% is achieved for neutrons without Gd.

4. Hopefully enough PMT hits to do any kind of analysis on (also based on the avg. PMT hits plots)

Higher PC would increase the efficiency but the costs/logistics need to be taken into consideration too. For even lower costs and less logistics, one could consider 8% PC with the PMT hit trigger threshold of 5. In such case,

1. **For Electrons:** > 6 MeV electrons are readily visible with trigger efficiency in the 90%’s while lower energies down to 2 MeV are still visible but at a reduced rate.

2. **For Gammas:** Detection is still possible at around 65% for energies > 6 MeV while trigger efficiency for energies lower than that is reduced nearly linearly until 2 MeV in which no detection is possible.

3. **For Neutrons with 0.1 Gd added:** Trigger efficiency of around 50%.

4 Particle Discrimination

In this final section, some event analysis is presented with another question looked into of *Can we differentiate particles, in particular neutrons, gammas, and electrons, in any way, and if so, how well?*

4.1 Bonsai

A tool that we will first need in order to do analysis is Bonsai^[5]. Bonsai is an algorithm originally used in the Super Kamiokande experiment for low energy neutrinos to calculate useful event quantities. Here we mostly just care about the reconstructed event vertex which will be used later. The idea of the algorithm is that we use the fact that low energy electrons and positrons don’t travel far (so we don’t need to consider track length) and then with PMT hit times, we use a maximum likelihood fitting based on,

$$\mathcal{L}(\mathbf{x}, t_0) = \sum_{i=1}^N \log(P(t - t_{tof} - t_0))$$

where t is the hit timing, t_{tof} is the time-of-flight from the vertex position to the hit PMT, t_0 is the time of the interaction, \mathbf{x} is the vertex position, and $P(t - t_{tof} - t_0)$ is the probability density function of the timing for a single photoelectron signal which was obtained from a LINAC.

4.2 Cherenkov Angle Algorithm

Now to review Cherenkov radiation which is used for the following event analysis algorithm. Cherenkov radiation occurs when a charged particle moves through a dielectric medium at a speed greater than the phase velocity (speed of propagation

of a wavefront in a medium) of light in that medium. A good comparison for Cherenkov radiation is to a sonic boom. The refractive index of water is usually around 1.33 so the charged particle needs to move faster than about $0.75c$. Electrons with energies >1 MeV, as simulated here, will be considered relativistic in which $\beta = v/c$ is roughly 1. We have then,

$$\cos(\theta_C) = \frac{1}{n\beta} \Rightarrow \theta_C = \cos^{-1}(1/1.33) \approx 42^\circ$$

from which a Cherenkov ring on the PMTs from an event will generally follow. Below in Fig. 14 is a good example of an event producing a Cherenkov ring that we can clearly see.

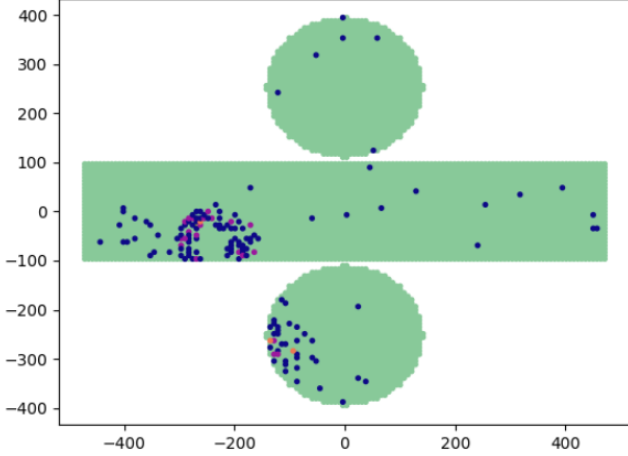


Fig. 14: A Cherenkov ring from simulation (using a very high pc of 90%)

Cherenkov radiation allows us not only to see charged particles in the detector but also can be used for a basic particle discrimination algorithm^[5]. Such an algorithm used here tries to gather the Cherenkov angle by obtaining the opening angle for all PMT triplet hits. The only variables needed are the Bonsai reconstructed vertex and PMT hit locations and timings. From this, we also get a measure of the isotropy of PMT hits per event. Completely isotropic events that don't actually create a single, real Cherenkov ring should give angles near 90 degrees. In particular, neutrons would hopefully be more isotropic and distinct from single gammas and electrons given that neutrons captured on Gd produce multiple gammas. This allows for a neutron discrimination then. Another note is that the electrons generated are quite low energy so they may not exactly produce angles of 42 degrees and instead will likely be more varied due to scattering. Meanwhile, a gamma would produce an even lower energy electron after a Compton scattering event. Overall, possible limiting factors for the algorithm include the low energies and small detector size. For instance, Super-K uses a cut of the reconstructed vertex being 2 m from the detector wall for similar analysis.

Method for Determining Opening Angle:

1. From a single particle event, read all PMT hits and get respective (x,y,z) positions of PMTs
2. Get initial particle vertex (via true position or Bonsai) and then the unit vectors from the vertex to the PMT hit positions (a projection onto the unit sphere around the vertex).
3. Of all possible 3 PMT hit combinations, the triplet should

create a circular cross section on the unit sphere defined by a cone with the vertex at the cone apex.

4. Calculate the radius of this circle using the Law of Sines.
5. With the radius of the circle and the fact that the cone slanted heights/sides are unit length, get the opening angle with arcsin and put it into a histogram.
6. (If the triangle area of the 3 unit PMT hit vector positions is too small (< 0.1) then the calculated angle is not put into the triplet angle histogram)
7. Repeat above steps for all PMT hit triplet combinations.
8. Now with the filled histogram (like in Fig. 15 for example), the most frequent angle is finally taken as the Cherenkov angle.

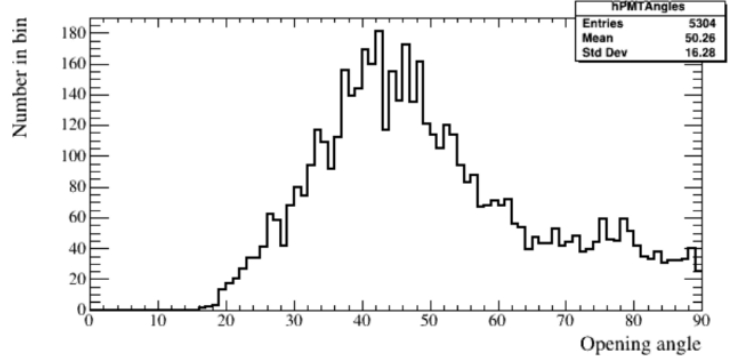


Fig. 15: Example of all triplet angles for a 4 MeV electron using the true vertex from detector center, 30% PC. From this, the final Cherenkov angle would be given as around 41 degrees

Now using the obtained final Cherenkov angle for particle discrimination, just generating events uniformly throughout detector with a low PMT hit threshold of 5 performs poorly at 30% PC (as neutrons with 0.1% wt Gd still give a sizable peak around 42 degrees). However, generating events more towards the center of the detector as well as using a higher PMT threshold helps. A possible explanation for this is that not all of the multiple gammas from the neutron capture on Gd are being picked up with the low hit threshold/PC and in addition, the neutron generated near the edge of the detector would increase this chance of one of the gammas escaping.

Overall then, using

- The Bonsai reconstructed vertex
- 30% PC
- Spatially uniform generation in the detector
- A 35 PMT hit count threshold
- A $\sqrt{x^2 + y^2} < 1$ m and $|z| < 0.5$ m cut for the reconstructed vertex
- Standard trigger (15 ns trigger window, 5 ns pre-trigger time, 50 ns post-trigger time, only recording the first PMT hit in a trigger window)

we get the following Figs. 16 through 18 for the neutrons, gammas and electrons:

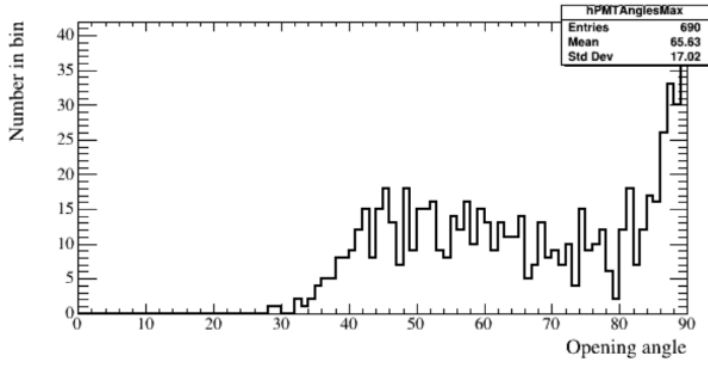


Fig. 16: Neutrons with initial energy of 6 MeV with 0.1% wt Gd

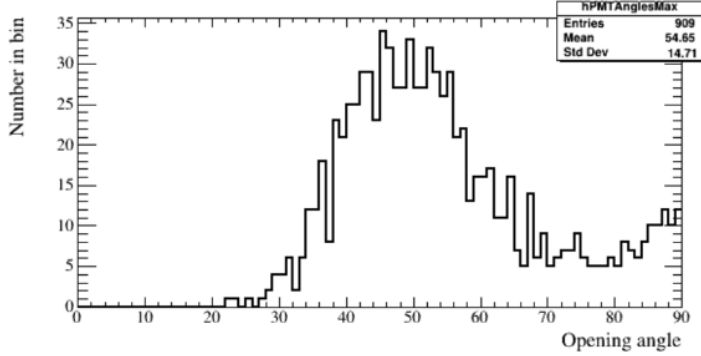


Fig. 17: Gammas with initial energy of 6 MeV

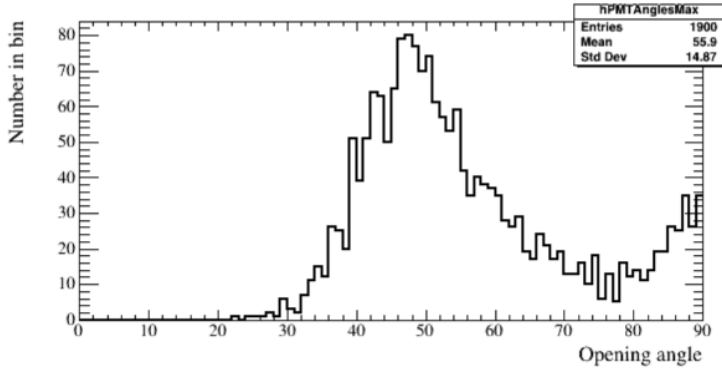


Fig. 18: Electrons with initial energy of 6 MeV

The takeaway from the three plots above is that we can distinguish between neutrons and gammas/electrons at a reduced event rate. Using a basic measure of performance, we consider the number of events that are triggered on out of the 10,00 generated and the number of events in the 30 to 55 degree opening angle range for each of the above three plots:

	Neutron w/Gd	Gamma	Electron
# Triggered On	690	909	1900
% Triggered On	6.9%	9.09%	19.0%
# between 30-50	212	537	1114

Therefore, disregarding the relative frequency that a particle would be realistically produced in the detector and instead generating the same number of all three particles, for events that we see passing the trigger, we can correctly identify it as not a neutron 88.7% percent of the time.

In combination with the Cherenkov algorithm so far, maybe via a likelihood method to improve performance, we could also consider shape analysis of the triplet histogram (with the simplest first thing being RMS as electron/gamma histograms tend to be more Gaussian-like while neutron histograms are often more sigmoid-like) and other variables like the mean and RMS of Bonsai reconstructed direction.

4.3 MSG Algorithm

The next natural question to ask is *Can we additionally discriminate between gamma and electron?*

The MSG (multiple scattering goodness) algorithm^[5] tries to look this by using the main difference between gammas and electrons particle events which is the degree of total scattering. Both will generally give off Cherenkov radiation with the electron by nature and the gamma by producing an energetic electron after a Compton scattering event. However, gammas are more likely to produce lower energy electrons which will tend to scatter more in the detector.

Small Explanation of the (simple) MSG Algorithm:

1. Looking at all pairs of PMT hits, project a Cherenkov cone based on the reconstructed vertex onto each (42 degree opening angle) and find all “cross points” of which there could be 0, 1, or 2. See Fig. 19.

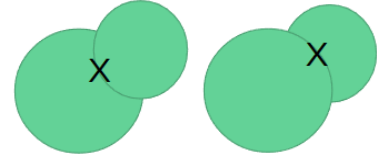


Fig. 19: Two Cherenkov ring cone projections where the “cross points” are the X’s

2. Take the unit vectors from the vertex to the “cross points” and group them into clusters within 50 degrees of an initial vector.
3. Add all the vectors in a cluster.
4. Take the largest vector sum of all the clusters and normalize it. This will be the new initial unit vector in step 3. Now repeat from step 2 for a number of iterations.
5. After a final iteration, take the largest vector sum before normalizing and divide that by the number of unit vectors obtained in step 2. This will give a final goodness value between 0 (more scattering) and 1 (less scattering).

Thus, below in fig. 20 and 21 are the MSG results for uniformly generated events in detector, using the true vertex and a 30 trigger PMT hit threshold with other standard trigger settings:

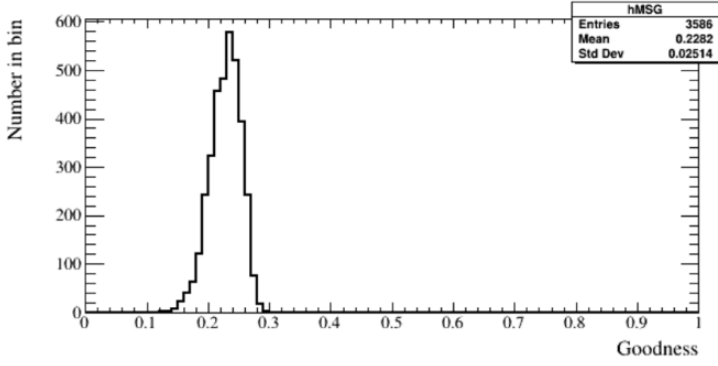


Fig. 20: 10 MeV gamma events

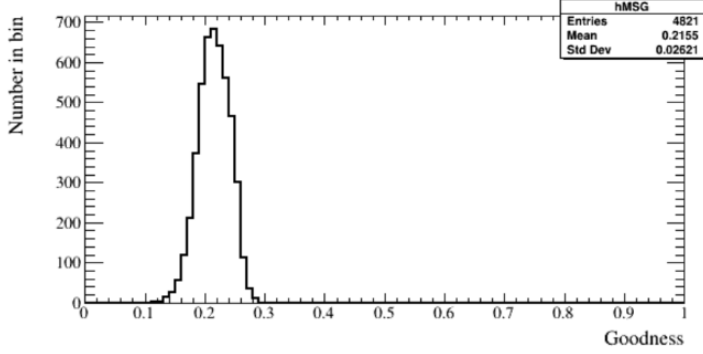


Fig. 21: 10 MeV electron events

The conclusion was that there was no clear distinction between the two, likewise when examining 6 MeV and some other cases. Even 4.6 MeV vs 8.4 MeV electrons using LINAC data in SK

differ only slightly though. However, one could still try more intricate steps in the MSG algorithm (like a Hough transform, shrinking cluster angle each iteration, etc).

4.4 Other Possible Methods of Particle Discrimination

A final note on the analysis presented here is that other methods of particle discrimination, in addition to refinement of the above work, could be developed and used for more ideal particle identification. Use of neural networks is one obvious choice but more sophisticated, subtler methods could also likely be utilized.

5 Report Conclusion and Acknowledgements

Above then is most of the work from the 2023 summer research internship I experienced at the University of Tokyo but there still is a lot more that could be done in terms of simulation work and of course the actual execution of the SNS experiment that's in the works. Overall, UTRIP was an unforgettable, amazing experience and so I would like to thank the people who made it happen. Thanks to UTRIP program coordinators along with the Yokoyama-Nakajima research group, in particular Yasuhiro Nakajima who was my professor advisor for the program. Finally, thanks to Emma who was also a UTRIP participant working in the same physics group. It was truly a pleasure to meet and work with everyone.

6 References

- [1] K. Hirata et al. (Kamiokande-II collaboration), Phys. Rev. Lett. 58, 1490 (1987).
- [2] COHERENT Collaboration. "A D2O detector for flux normalization of a pion decay-at-rest neutrino source" JINST 16 (2021) 08. 2104.09605
- [3] S. Agostinelli et al. (GEANT4). "GEANT4—a simulation toolkit." Nucl. Instrum. Meth. A 506, 250–303 (2003).
- [4] <https://github.com/WCSim>
- [5] More info on Bonsai, Cherenkov angle reconstruction and MSG can be found in many PhD theses such as:
 - Bonsai/MSG (section 5.1/6.5)=https://www-sk.icrr.u-tokyo.ac.jp/sk/_pdf/articles/Renshaw_Doctoral_Thesis.pdf
 - Cherenkov (section 5.4)=https://www-sk.icrr.u-tokyo.ac.jp/sk/_pdf/articles/doctor_edited_iida.pdf